Exchange bias effect and intragranular magnetoresistance in $Nd_{0.84}Sr_{0.16}CoO_3$

2009 J. Phys.: Condens. Matter 21 486003

(http://iopscience.iop.org/0953-8984/21/48/486003)

J. Phys.: Condens. Matter **21** (2009) 486003 (6pp) doi:10.1088/0953-8984/21/48/486003

Exchange bias effect and intragranular magnetoresistance in $Nd_{0.84}Sr_{0.16}CoO_3$

M Patra, S Majumdar and S Giri

Department of Solid State Physics, Indian Association for the Cultivation of Science, Jadavpur, Kolkata 700 032, India

E-mail: sspsg2@iacs.res.in

Received 25 August 2009, in final form 8 October 2009
Published 6 November 2009
Online at stacks.iop.org/JPhysCM/21/486003

Abstract

Electrical transport properties as a function of magnetic field and time have been investigated in polycrystalline, $Nd_{0.84}Sr_{0.16}CoO_3$. A strong exchange bias (EB) effect is observed associated with the fairly large intragranular magnetoresistance (MR). The EB effect observed in the MR curve is compared with the EB effect manifested in the magnetic hysteresis loop. A training effect, described as the decrease of EB effect when the sample is successively field cycled at a particular temperature, has been observed in the shift of the MR curve. The training effect could be analyzed by successful models. The EB effect, MR and a considerable time dependence in MR are attributed to the intrinsic nanostructure giving rise to varieties of magnetic interfaces in the grain interior.

(Some figures in this article are in colour only in the electronic version)

1. Introduction

Since the evidence of spin-polarized electron transport [1], followed by the discovery of giant magnetoresistance (GMR) in layered magnetic multilayer films [2, 3], a twist in conventional electronics has been experienced and a new field in electronics, namely spintronics, has arisen. Spintronics or spin electronics is a multidisciplinary field where the manipulation of spin degrees of freedom has been exploited in solid state electronics [4, 5]. Spintronics involving GMR, tunnel magnetoresistance (TMR), and exchange bias (EB) effects has attracted considerable attention in the last decade. In particular, a new generation of spintronic devices have been designed such as magnetoresistive random access memory and spin valve sensors.

The exchange bias phenomenon was initially reported in a heterogeneous system composed of ferromagnetic (FM) and antiferromagnetic (AFM) substances manifested by the shifts in the magnetic hysteresis loop when the system is cooled through the Néel temperature [6]. Since the discovery of the exchange bias effect it has been noticed in varieties of combination between soft and hard magnetic substances e.g. FM, AFM, spin-glass (SG), cluster-glass (CG) and ferrimagnetic (FI) systems [7–10]. The EB effect has also been evidenced through the systematic shifts in magnetoresistance–field (MR–H) curve which are limited to the bilayer or multilayer films only [11–14]. Recently, the EB effect has been reported in a few compounds as being attributed to the grain interior spontaneous phase separation where EB effect was reported through the shift in the magnetic hysteresis loop [9, 10, 15–19]. In this paper, we report a new paradigm of the EB effect in a polycrystalline compound, $Nd_{0.84}Sr_{0.16}CoO_3$ through the shifts in the MR–H curve. We observe the strong EB effect involved with a fairly large intragranular MR where the value of EB field is found to be much larger than the observation measured through the shift in the magnetic hysteresis loop. Furthermore, we observe a training effect in the shift of the MR–H curve which is in accordance with the successful models used to interpret the training effect observed in the magnetic hysteresis loop. A strong time dependence in the resistivity is observed at low temperature which is found to be correlated with the EB effect. Finally, we propose a possible scenario of grain interior magnetic nanostructure to interpret the new magnetotransport behavior involved with the EB effect.

The hole doped compound, $Nd_{1-x}Sr_xCoO_3$ exhibits different characteristic features depending on the degree of hole doping [20]. For the low doping range a SG or CG state has been proposed with a resistivity showing a semiconducting temperature dependence. With a further increase in hole doping the short range FM clusters begin to coalesce above a percolation threshold ($x > 0.18$) to attain

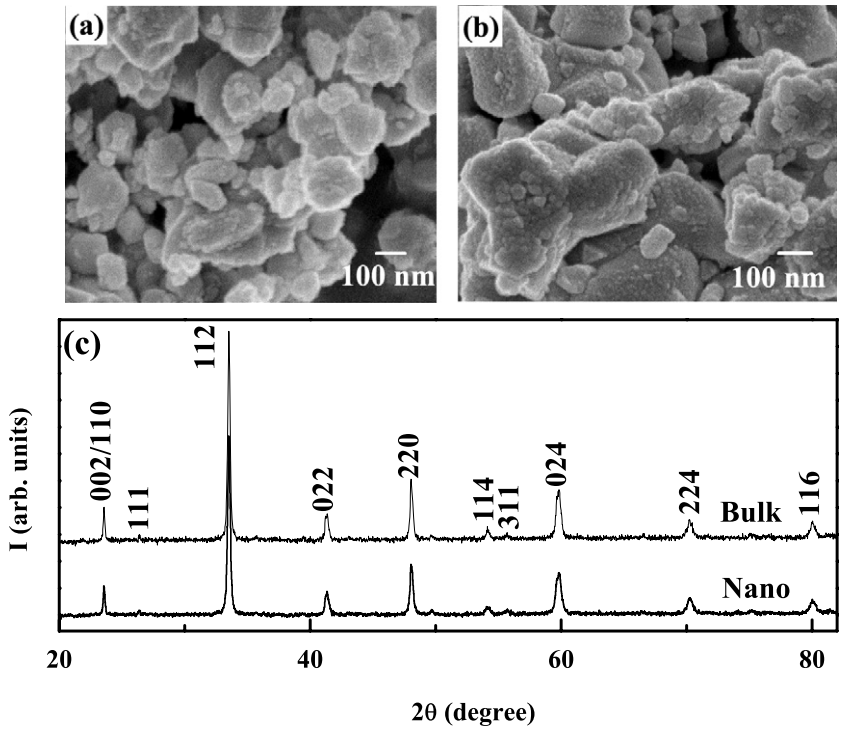

Figure 1. SEM images for the nanoparticle (a) and bulk (b). Powder x-ray diffraction patterns are shown in (c) for the nanoparticle and bulk.

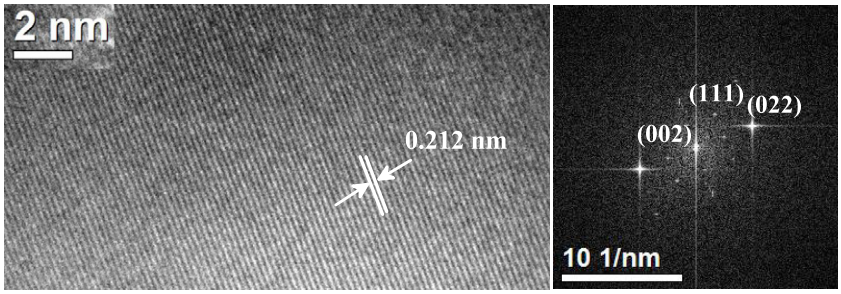

Figure 2. HRTEM image (left panel) and corresponding FFT image (right panel) for the bulk sample.

magnetic long range ordering and the material shows metallic conductivity in the ordered state. The coexistence of FI and FM ordering is reported for the compounds above and close to the percolation threshold. Neutron powder diffraction studies on $Nd_{0.67}Sr_{0.33}CoO_3$ confirm the coexistence of FM and FI ordering where ferrimagnetism was interpreted in terms of an induced antiparallel ordering of the Nd spins in close proximity to the Co sublattice [21]. In the present investigation we note that a convincing feature of the EB effect in the MR–H curve is observed at $x = 0.16$, which is close to the percolation threshold.

2. Synthesis and structural characterization

The polycrystalline compound with composition $Nd_{0.84}Sr_{0.16}CoO_3$ was prepared by the sol–gel technique [9]. The preheated samples were finally annealed at 1073 and 1273 K with average grain sizes ∼100 and ∼200 nm, respectively, as confirmed by scanning electron microscopy using a JEOL FESEM microscope (JSM-6700F). The grain sizes of the samples are shown in figures 1(a) and (b). For simplicity, we address the sample with larger grain size as bulk while the sample with smaller grain size is defined as the nanoparticle. The single phase orthorhombic structure ($Pbnm$) was confirmed for both the samples by a powder x-ray diffractometer (Seifert XRD 3000P) using Cu Kα radiation. Figure 1(c) exhibits the x-ray diffraction patterns for the nanoparticle and bulk, respectively. In order to check any microstructural inhomogeneities in the grain interior, high resolution transmission electron microscopy (HRTEM) was carried out on the bulk using a JEOL TEM, 2010 microscope. We have checked several portions of different particles randomly and they do not show any structural inhomogeneities. An example of an HRTEM image is shown in the left panel of figure 2 exhibiting a single lattice fringe. The lattice spacing of the observed plane is ∼0.212 nm, which matches with the spacing (∼0.218 nm) of the (202) plane of the orthorhombic structure ($Pbnm$) having lattice constants, $a = 0.534$ nm,

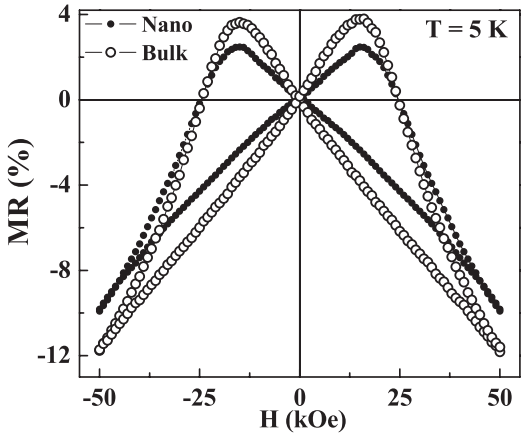

Figure 3. MR–H curves for bulk and nanoparticles at 5 K while the sample was cooled down to 5 K in zero field.

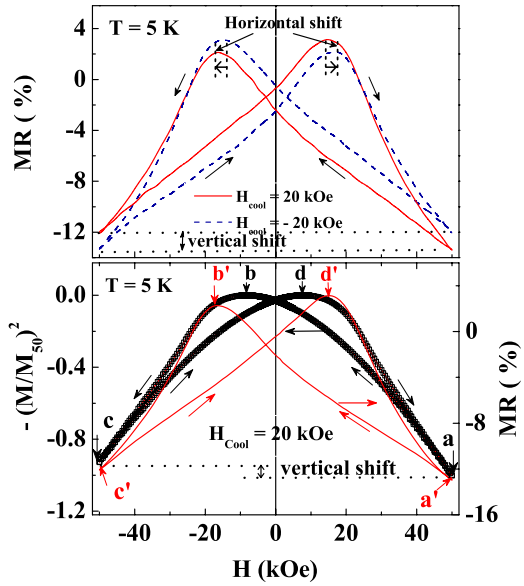

Figure 4. Top panel: MR–H curves for $H_{\rm cool} = \pm 20$ kOe displaying the vertical and horizontal shifts. Bottom panel: $-(M/M_{50})^2$–H and MR–H curves with $H_{\rm cool} = 20$ kOe for comparing the magnetic and magnetoresistance results.

$b = 0.533$ nm, and $c = 0.757$ nm, as obtained from the powder x-ray diffraction patterns. A two-dimensional fast Fourier transform (FFT) of the lattice resolved image is shown in the right panel of figure 2 and this can be indexed to the orthorhombic structure. The magnetic field dependence of resistivity (ρ), using the four-probe method and magnetization (M), were determined on pelletized samples using a cryogen-free physical property measurement system (Cryogenic Ltd, UK).

3. Results and discussions

3.1. Intragranular magnetoresistance and exchange bias effect

The magnetoresistance (MR) is defined as $(\rho_H - \rho_0)/\rho_0$, where ρ_H and ρ_0 are the resistivities in a static and zero field, respectively. A symmetric MR–H curve (open symbol) at 5 K having a fairly large MR ($\sim$ 12%) at 50 kOe is shown in figure 3 for the bulk. The peak in the MR–H curve exhibits a typical manifestation of the tunneling mechanism. Tunneling between ferromagnetic (FM) grains across the grain boundary region has been commonly interpreted in polycrystalline materials [22]. Since the grain boundary region is considerably enhanced by decreasing the grain size than for the bulk counterpart, the MR should increase considerably due to the decrease in average grain size if the grain boundary effect is the dominant factor. The MR–H curve at 5 K was also measured for the nanoparticle, depicted by the closed symbols in figure 3. For the nanoparticle the MR decreases considerably, suggesting that the grain boundary effect does not contribute any significant role. Rather, it is a mechanism of the grain interior that causes the change in MR. A short range FM and metallic clusters embedded in the non-FM matrix in the grain interior have been proposed by Stauffer *et al* in $Nd_{1-x}Sr_xCoO_3$, where the density and size of the short range FM clusters increase with hole (Sr) doping [20]. Thus, we propose that MR is involved with the tunneling between metallic FM clusters across the non-FM matrix, analogous to that observed in the identical spontaneously phase separated cobaltite, $La_{1-x}Sr_xCoO_3$ [23, 24]. The results are also similar to the negative intergranular MR previously observed in artificial structures composed of nanoscale FM particles embedded in an insulating or metallic nonmagnetic matrix, where the orientation of the magnetization axes, the density, and the size of the FM entities are crucial to interpreting the tunneling magnetoresistance effect [25–27]. Note that the matrix itself is magnetic in the present observation. Since the matrix component is highly anisotropic ferrimagnetic, the high field response of the MR is expected as being mainly due to the polarization of the ferrimagnetic matrix. In addition to TMR, an asymmetry in the MR–H curve is strikingly observed along with the convincing shifts in the vertical and horizontal axes (top panel of figure 4) when sample was cooled down to 5 K from room temperature in a cooling field, $H_{\rm cool} = 20$ kOe. We further note that shifts are present in the magnetic hysteresis loop when the sample was cooled under similar conditions. MR and $(M/M_{50})^2$ with H are plotted together in the bottom panel of figure 4, where M_{50} is the magnetization (M) at $H = 50$ kOe. The asymmetry in the MR–H and $(M/M_{50})^2$–H curves are typical manifestations of the EB effect. The measurements were carried out at $x = 0.12$, 0.16, and 0.18, and the EB effect is found to be largest at $x = 0.16$, which is close to the percolation threshold of conductivity as well as long range FM ordering.

Peaks are typically observed in the MR–H curve at $M = 0$ for TMR, where the magnetic field at the peak position determines the coercivity [22]. Here, the average value of the field at the peaks in MR is observed at $H_C' = 15.5$ kOe, which is almost twice the coercivity ($H_C = 8.0$ kOe) obtained from the magnetic hysteresis loop. The peaks in the MR–H and $(M/M_{50})^2$–H curves, from which the coercivities are estimated, are illustrated by the arrows at b′, d′, b, and d in the bottom panel of figure 4. The magnetoelectric phase diagram [20] and neutron diffraction [21] confirm that short

range FM clusters are embedded in the ferrimagnetic (FI) matrix close to the percolation limit. If the system consists of FM and FI substances, bulk magnetic measurements provide the average coercivity of FM and FI components. It is recognized that the coercivity of the FM compound is typically much smaller than the anisotropic FI compound. Here, TMR is involved with the tunneling between metallic FM clusters across the semiconducting FI matrix where the tunneling barrier is set by the anisotropy of the FI spins. Thus, the coercivity noticed in MR–H curve provides the coercivity of the individual FI component. A similar argument has been proposed in the double perovskite, Sr_2FeMoO_6, where a nearly six times larger coercivity in MR was observed than that of the value obtained from the magnetic hysteresis loop [28].

If H_b and H_d are the negative and positive coercivities indicated by the arrows at peaks b and d, respectively, the EB field (H_E) is defined as $H_E = |H_b - H_d|/2 \approx 250$ Oe. The exchange bias field (H_E^{MR}) obtained from the MR–H curve is $H_E^{MR} = |H_{b'}^{MR} - H_{d'}^{MR}|/2 \approx 744$ Oe, where $H_{b'}^{MR}$ and $H_{d'}^{MR}$ correspond to the fields at peaks b′ and d′, respectively depicted in the bottom panel of figure 4. Interestingly, H_E^{MR} is significantly much higher than H_E. Theoretical interpretations [29, 30] seem to agree with the conclusion that the EB effect should be stronger for a larger anisotropy of the hard magnetic substance. Here, $H_E^{MR} \gg H_E$ is in accordance with the proposed theories [29, 30]. We note in the top panel of figure 4 that the vertical and horizontal shifts in MR are opposite while the direction of H_{cool} is opposite. The peak position in the MR–H curve measured from 50 to −50 kOe is shifted toward the negative direction along with a considerable decrease in the height of the curve, while the curve measured from −50 to 50 kOe remains almost unaltered for $H_{cool} = 20$ kOe. The opposite feature is illustrated in the top panel of figure 4 for $H_{cool} = -20$ kOe. The results clearly demonstrate a spin valve-like character in MR analogous to that reported in bilayer or multilayer films [11, 14, 13].

3.2. Training effect in the magnetoresistance curve

The training effect (TE) is one of the significant manifestations of the EB effect which describes the decrease of the EB effect when the sample is successively field cycled at a particular temperature. The TE is typically observed in the magnetic hysteresis loop [7] which has been recently reported in the MR–H curve of only two multilayer films, exhibiting the EB effect [31, 32]. In figure 5 a typical signature of the TE is illustrated at 5 K up to 5 successive cycles (λ). The decrease of the shift of peak positions along the negative field axis is highlighted in the left inset of the figure. A large decrease of $H_E^{MR} \sim 33\%$ is observed between the first and second cycles. The decrease of H_E^{MR} is fitted satisfactorily (solid straight line) with the empirical relation, $H_E^{MR}(\lambda) - H_E^{MR}(\lambda = \infty) \propto \frac{1}{\sqrt{\lambda}}$ for $\lambda \geqslant 2$ with $H_E^{MR}(\lambda = \infty) \approx 100$ Oe. The empirical relation does not fit the sharp decrease between the first and second cycles, in accordance with the reported results in the magnetic hysteresis loop [7] as well as MR–H curve [31]. Binek proposed a recursive formula in the framework of a spin

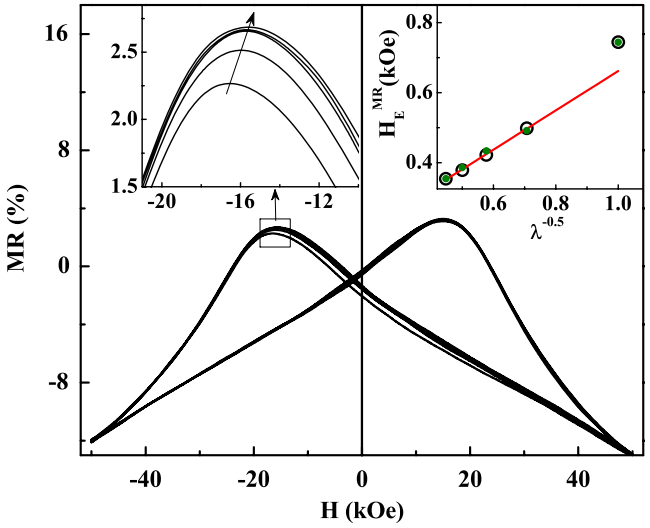

Figure 5. The training effect is shown in the MR–H curves up to 5 successive cycles (λ = 5). (Left inset) highlights the shift of peak position with increasing λ, where the arrow indicates the increasing direction of λ. (Right inset) Plot of H_E with $\lambda^{-0.5}$, where the solid straight line exhibits the fit by a power law. Open circles are the experimental data while small filled symbols represent the simulated data described in equation (1).

configurational relaxation model to interpret the training effect which correlates the (λ+1)th loop shift with the λth one as [33]

$$H_E^{MR}(\lambda + 1) - H_E^{MR}(\lambda) = -\gamma[H_E^{MR}(\lambda) - H_E^{MR'}(\lambda = \infty)]^3 \quad (1)$$

where γ is a sample dependent constant. Using $\gamma = 8.3 \times 10^{-7}$ Oe^{-2} and $H_E^{MR'}(\lambda = \infty) = 71.87$ Oe, the whole set of data (filled circles) could be generated which match satisfactorily with the experimental data (open circles).

3.3. Time dependence in the resistivity

We note a considerable time (t) dependence in ρ at low temperature when sample was cooled down to 5 K from room temperature with $H_{cool} = 50$ kOe and then ρ was measured against time t after removal of magnetic field. The plot of $[\rho(t) - \rho(0)]/\rho(0)$ with t is illustrated in figure 6 (open circles). The relaxation follows a stretched exponential with a critical exponent (β). The value of β is $0 < \beta < 1$, when it is involved with the activation against distribution of anisotropy barriers typically observed in the relaxation of magnetization, exhibiting glassy magnetic behavior [34]. The satisfactory fit using a stretched exponential function, $[\rho(t) - \rho(0)]/\rho(0) = A + B\exp(t/\tau)^{\beta}$ is shown by the continuous curve in the figure, with a relaxation time, $\tau = 4374$ s and $\beta = 0.33$, suggesting glassy magnetic behavior in the transport properties. A very small t dependence of ρ is observed (filled circles) when the sample is cooled in zero field and the measurement is carried out in 50 kOe. The results clearly demonstrate that a strong t evolution of ρ is involved with field cooling which is correlated to the EB effect. The HRTEM image confirms the absence of any structural inhomogeneities in the grain interior of the compound, which indicates that

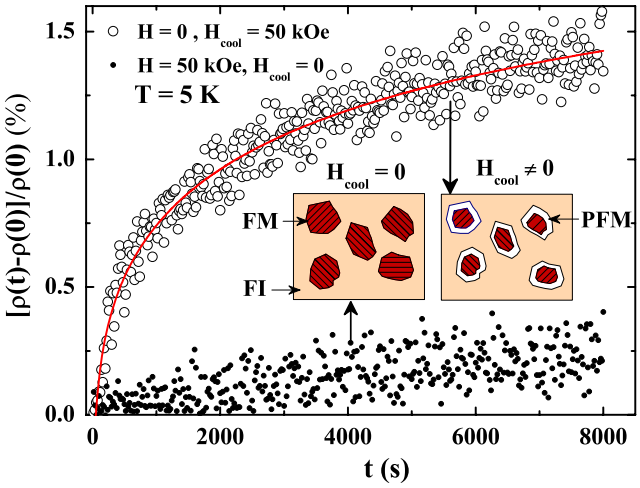

Figure 6. Time (t) evolution of $[\rho(t) - \rho(0)]/\rho(0)$ at 5 K measured in zero field (open symbols) and $H = 50$ kOe (filled symbols) after cooling in FC and ZFC modes, respectively. Inset shows diagrams of the grain interior magnetic nanostructure. FM, PFM and FI represent the FM, pinned FM and FI regions.

the grain interior nanostructure is purely magnetic in origin, in accordance with the previous reports [20, 21]. A diagram of the phase separation scenario within a grain is proposed in the left inset of figure 6 where short range FM regions or clusters are embedded in the FI matrix. $\rho(t)$ measured in two different conditions is illustrated in the figure while vertical arrows represent the corresponding grain interior magnetic nanostructure. When the sample is cooled in field, a new layer consisting of pinned ferromagnetic (PFM) spins arises at the FM/FI interface due to the pinning of the soft FM spins by the hard FI spins. The appearance of a new layer comprising of PFM spins leads to the strong t dependence in ρ. We further note that the t dependence of ρ could be satisfactorily analyzed by a stretched exponential which has been typically used to characterize the glassy magnetic behavior. Thus, strong t dependence as well as satisfactory fit by the stretched exponential suggest the glassy magnetic behavior of the PFM spins which has been revealed in the transport properties. Furthermore, the PFM layer having unidirectional anisotropy gives rise to a unidirectional shift in the MR–H curve, where the polarization direction of PFM spins are strongly influenced by the direction of the cooling field leading to the EB effect and spin valve-like mechanism in the MR.

4. Conclusions

In this paper we report a new observation of the EB effect in a compound attributed to the grain interior intrinsic nanostructure where the EB is observed through the measurements of magnetoresistance analogous to that observed in the bilayer or multilayer films. The training effect in the shift of the magnetoresistance curve further confirms the evidence of the EB effect where the training effect could be analyzed with successful models. The EB effect is found to be substantially larger than the effect observed in the magnetic hysteresis loop where a stronger EB effect is correlated to the stronger coercivity in MR than the magnetic measurements. A strong time dependence in the resistivity, exhibiting glassy magnetic behavior, is observed due to field cooling which is correlated to the EB effect. A possible scenario of the grain interior nanostructure has been suggested to interpret the experimental results in polycrystalline $Nd_{0.84}Sr_{0.16}CoO_3$, where the grain interior nanostructure is close to the percolation threshold.

Acknowledgments

SG wishes to thank DST (Project No. SR/S2/CMP-46/2003), India for financial support. MP thanks CSIR, India for a fellowship.

References

[1] Johnson M and Silsbee R H 1985 *Phys. Rev. Lett.* **55** 1790
[2] Baibich M N, Broto J M, Fert A, Van Dau Nguyen F and Petroff F 1988 *Phys. Rev. Lett.* **61** 2472
[3] Binasch G, Grünberg P, Saurenbach F and Zinn W 1989 *Phys. Rev.* B **39** 4828
[4] Prinz G A 1998 *Science* **282** 1660
[5] Gregg J F 2007 *Nat. Mater.* **6** 798
[6] Meiklejohn W H and Bean C P 1956 *Phys. Rev.* **102** 1413
[7] Nogues J, Sort J, Langlais V, Skumryev V, Surinach S, Munoz J S and Baro M D 2005 *Int. J. Nanotechnol.* **2** 23
Nogues J and Schuller I K 1999 *J. Magn. Magn. Mater.* **192** 203
[8] Iglesias O, Labarta A and Batlle X 2008 *J. Nanosci. Nanotechnol.* **8** 2761
[9] Patra M, Majumdar S and Giri S 2009 *J. Phys.: Condens. Matter* **21** 236004
[10] Patra M, Majumdar S and Giri S 2009 *Solid State Commun.* **149** 501
[11] Nikolaev K R, Krivorotov I N, Cooley W K, Bhattacharya A, Dan Dahlberg E and Goldman A M 2000 *Appl. Phys. Lett.* **76** 478
[12] Kerr E, Dijken S van and Coey J M D 2005 *J. Appl. Phys.* **97** 093910
[13] Dai N V, Thuan N C, Hong L V, Phuc N X, Lee Y P, Wolf S A and Nam D N H 2008 *Phys. Rev.* B **77** 132406
[14] Béa H, Bibes M, Cherifi S, Nolting F, Warot-Fonrose B, Fusil S, Herranz G, Deranlot C, Jacquet E, Bouzehouane K and Barthélémy A 2006 *Appl. Phys. Lett.* **89** 242114
[15] Patra M, De K, Majumdar S and Giri S 2007 *Eur. Phys. J.* B **58** 367
[16] Thakur M, Patra M, De K, Majumdar S and Giri S 2008 *J. Phys.: Condens. Matter* **20** 195215
[17] Niebieskikwiat D and Salamon M B 2005 *Phys. Rev.* B **72** 174422
[18] Tang Y K, Sun Y and Cheng Z H 2006 *Phys. Rev.* B **73** 174419
[19] Huang W G, Zhang X Q, Du H F, Yang R F, Tang Y K, Sun Y and Cheng Z H 2008 *J. Phys.: Condens. Matter* **20** 445209
[20] Stauffer D D and Leighton C 2004 *Phys. Rev.* B **70** 214414
[21] Krimmel A, Reehuis M, Paraskevopoulos M, Hemberger J and Loidl A 2001 *Phys. Rev.* B **64** 224404
[22] Coey J M D 1999 *J. Appl. Phys.* **85** 5576
[23] Wu J, Lynn J W, Glinka C J, Burley J, Zheng H, Mitchell J F and Leighton C 2005 *Phys. Rev. Lett.* **94** 037201
[24] Patra M, Majumdar S and Giri S 2009 *Europhys. Lett.* **87** 58002
[25] Xiao J Q, Jiang S J and Chien C L 1992 *Phys. Rev. Lett.* **68** 3749

[26] Barzilai S, Goldstein Y, Balberg I and Helman J S 1981 *Phys. Rev.* B **23** 1809
[27] Sankar S, Berkowitz A E and Smith D J 2000 *Phys. Rev.* B **62** 14273
[28] Sarma D D, Ray S, Tanaka K, Kobayashi M, Fujimori A, Sanyal P, Krishnamurthy H R and Dasgupta C 2007 *Phys. Rev. Lett.* **98** 157205
[29] Meiklejohn W H 1962 *J. Appl. Phys.* **33** 1328
[30] Weinberger P 2007 *Phys. Rev.* B **75** 064405
[31] Ventura J, Araujo J P and Sousa J B 2008 *Phys. Rev.* B **77** 184404
[32] Brems S, Buntinx D, Temst K, Van Haesendonck C, Radu F and Zabel H 2005 *Phys. Rev. Lett.* **95** 157202
[33] Binek Ch 2004 *Phys. Rev.* B **70** 014421
[34] Mydosh J A 1993 *Spin Glasses: An Experimental Introduction* (London: Taylor and Francis)